

## PREPARATION AND STRUCTURE REFINEMENT OF SYNTHETIC $Ti^{3+}$ -CONTAINING LINDSLEYITE, $BaMn_3Ti_{18}O_{38}$

RONALD C. PETERSON\* AND IAN E. GREY

CSIRO, Division of Minerals, P.O. Box 124, Port Melbourne, Victoria, 3207, Australia

### ABSTRACT

The stability field for lindsleyite in the system  $BaO-MnO-TiO_2-Ti_2O_3$  at 1100°C was studied using the quench method with  $H_2-CO_2$  gas mixtures to control the oxygen fugacity. Lindsleyite is stable at oxygen fugacities lower than  $10^{-14.5}$  atm., down to the lowest fugacity used,  $10^{-17.5}$  atm. A lindsleyite phase with composition  $BaMn_3Ti_{18}O_{38}$  was prepared at an oxygen fugacity of  $10^{-15.7}$  atm. for structural studies. The phase contains trivalent titanium, with  $Ti^{3+}:Ti^{4+} = 4:14$ . It has rhombohedral symmetry,  $R\bar{3}$ , with  $a$  10.4369(1) and  $c$  20.8871(2) Å. A Rietveld refinement of the structure was made using powder X-ray-diffraction data. The twelve-coordinated A site is the largest observed for minerals of the crichtonite group. The mean A-O bond length is shown to have a linear relationship with the radii of the cations assigned to this site for all the minerals in the crichtonite group.

**Keywords:** lindsleyite, crichtonite group, powder diffraction, Rietveld structure refinement, trivalent titanium.

### SOMMAIRE

Nous avons étudié le champ de stabilité de la lindsleyite dans le système  $BaO-MnO-TiO_2-Ti_2O_3$  à 1100°C avec la méthode de trempe et une proportion variable des gaz  $H_2$  et  $CO_2$  pour contrôler la fugacité de l'oxygène  $f(O_2)$ . La lindsleyite serait stable à une valeur de  $f(O_2)$  inférieure à  $10^{-14.5}$  atmosphères, et le demeure jusqu'à la plus faible valeur de  $f(O_2)$  utilisée,  $10^{-17.5}$  atmosphères. Nous avons synthétisé la lindsleyite de composition  $BaMn_3Ti_{18}O_{38}$  à une valeur de  $f(O_2)$  de  $10^{-15.7}$  atmosphères pour notre étude structurale. Ce composé contient du titane trivalent, et la proportion  $Ti^{3+}:Ti^{4+}$  serait 4:14. Il possède une symétrie rhomboédrique,  $R\bar{3}$ ,  $a$  10.4369(1),  $c$  20.8871(2) Å. Un affinement de sa structure a été effectué sur données diffractométriques (méthode des poudres) par méthode de Rietveld. Le site A à coordinence douze est le plus gros qui soit connu pour les membres du groupe de la crichtonite. Parmi les membres de ce groupe, la dimension A-O moyenne montre une relation linéaire avec le rayon des cations occupant ce site.

(Traduit par la Rédaction)

**Mots-clés:** lindsleyite, groupe de la crichtonite, diffraction X sur poudre, affinement de la structure, méthode de Rietveld, titane trivalent.

### INTRODUCTION

Lindsleyite was first identified by Haggerty (1975) from the DeBeers kimberlite in the Republic of South Africa and subsequently described by Haggerty *et al.* (1983). Lindsleyite is a member of the crichtonite group of minerals, which have the general formula  $AM_{19}T_2O_{38}$ . Here, A represents large 12-coordinated cations (Ba in lindsleyite), and M and T represent smaller cations such as Ti, Cr, Mn and Fe, with octahedral and tetrahedral coordination, respectively. Other minerals in this group are loveringite (A = Ca: Gatehouse *et al.* 1978), landauite (A = Na: Grey & Gatehouse 1978), senaite (A = Pb: Grey & Lloyd

1976), davidite (A = U + REE: Gatehouse *et al.* 1979), crichtonite (A = Sr: Grey *et al.* 1976) and mathiasite (A = K: Gatehouse *et al.* 1983, Lu & Peng 1987). Minerals in the lindsleyite-mathiasite series have been studied by Zhang *et al.* (1988, 1989) and by Jiang *et al.* (1990). These minerals are of interest as indicators of conditions of kimberlite formation. The crichtonite group of minerals have also been considered as a possible repository of nuclear waste-materials (Buykx *et al.* 1988).

The present study on synthetic lindsleyite evolved from work on modifications to the Becher process of upgrading ilmenite to allow removal of radionuclide impurities. The commercial Becher-type process involves reduction of the iron oxide content of ilmenite to the metal, followed by leaching to remove the metallic iron, and gives an upgraded titanate-rich product called synthetic rutile (Becher *et al.* 1965). The

\* Permanent address: Department of Geological Sciences, Queen's University, Kingston, Ontario K7L 3N6.

modified process, known as SREP (Synthetic rutile enhancement process: Ellis *et al.* 1994) involves the addition of flux during reduction to segregate the radionuclides and other impurities into a readily leachable phase. Laboratory testwork showed that under certain conditions of reduction, alkalis and alkaline earths in the fluxes reacted with the titanate to form small amounts of crichtonite-group phases. Under these conditions, there was the possibility that the radionuclide,  $Ra^{2+}$ , segregated into the *A* site of these phases. An investigation of the stability of this phase was made using  $Ba^{2+}$  to simulate the radioactive radium. Under the strongly reducing conditions used in Becher-type upgrading of Western Australian ilmenite, the iron oxide content of the ilmenite is converted to the metal, and manganese oxide,  $MnO$ , becomes the major stabilizing oxide in the reduced titanate phases. The experiments were thus defined by lindsleyite formation in the system  $BaO-MnO-TiO_2-Ti_2O_3$ , for oxygen fugacity and temperature conditions relevant to the upgrading of ilmenite.

## EXPERIMENTAL

### Phase studies

The stability field for lindsleyite in the system  $Ba-Mn-Ti-O$  at  $1100^\circ C$  under reducing conditions was determined by equilibration controlled in a gaseous atmosphere. Environments having a fugacity of oxygen in the range  $10^{-14.5}$  to  $10^{-17.5}$  atm. were established using  $H_2-CO_2$  mixtures. According to the published results of Suzuki & Sambongi (1972), this range of fugacity corresponds to the composition range  $TiO_{1.993}$  to  $TiO_{1.833}$  in the pure  $Ti-O$  system at  $1100^\circ C$ . These reduced compositions of rutile cover the range normally observed in the reduced products from commercial ilmenite-reduction kilns (Grey & Reid 1974). The lower limit of oxygen fugacity,  $10^{-17.5}$  atm., was set to avoid carbon deposition.

Starting materials for the equilibrations were analytical reagent (AR) grade  $BaCO_3$ ,  $MnO_2$  and  $TiO_2$  (anatase form). Some runs were carried out using  $Mn_2O_3$ , prepared by thermal decomposition of AR-grade  $MnCl_2 \cdot 4H_2O$  at  $600^\circ C$ . Weighed mixtures of the starting materials were pressed into pellets and heated for 16 h in the controlled atmosphere, then quenched in a high-purity nitrogen flow. All samples were subjected to at least two heat treatments, with intermediate fine grinding, to ensure that equilibrium was achieved. Further details of the apparatus and procedure used for studies in a controlled atmosphere are given by Grey *et al.* (1974).

### Electron-microprobe analyses

Wavelength-dispersion X-ray analyses on lindsleyite phases in polished thin sections were carried out

using a Cameca Camebax electron microprobe operated at 15 kV and 20 nA. Rutile,  $TiO_2$  ( $TiK\alpha$ ), manganese metal ( $MnK\alpha$ ) and benitoite,  $BaTiSi_3O_9$  ( $BaL\beta$ ) were used as standards. Particular care was taken to minimize errors due to overlap of barium and titanium peaks.

### Powder X-ray diffraction

Powder X-ray diffraction (PXRD) was used for the routine identification of phases in the equilibrated products and to provide intensity data for structure refinements by the Rietveld method (Rietveld 1969). Samples for PXRD were prepared by crushing then grinding equilibrated pellets in a tungsten carbide ball mill and back-pressing into an aluminum sample holder. Measurement of diffracted intensities was made using a Philips 1050 goniometer with a PW1710 controller using a long fine-focus Cu tube. The diffractometer was configured with a  $1^\circ$  divergent slit, 0.2 mm receiving slit,  $1^\circ$  scatter slit,  $5^\circ$  incident and diffracted beam Soller slits, and a diffracted-beam curved graphite monochromator.

For the Rietveld refinements, intensity data were collected at  $22^\circ C$ , from  $10^\circ$  to  $150^\circ 2\theta$ , with a step size of  $0.025^\circ$  and a variable counting-time strategy (Madsen & Hill 1994). The total counting time was 43.2 ks. Powder-diffraction step-scan intensities may be obtained from The Depository of Unpublished Data, CISTI, National Research Council of Canada, Ottawa, Ontario K1A 0S2.

### Rietveld refinement of $BaMn_3Ti_{18}O_{38}$

Least-squares refinements were carried out using the Rietveld program SR2, a local modification of the code by Hill & Howard (1986) and Wiles & Young (1981) that takes account of variable-time data sets. Profile-refinement parameters included a scale factor, two pseudo-Voigt shape parameters, a  $2\theta$  zero parameter, a three-term full-width at half-maximum function (Caglioti *et al.* 1958), calculated for nine half-widths on either side of the peak maxima, a peak-asymmetry parameter for peaks less than  $50^\circ 2\theta$ , and unit-cell parameters. The background was modeled using a five-parameter polynomial fit. Scattering curves for neutral atoms were taken from International Tables for X-ray Crystallography (1974).

The refinement was initiated using the reported atomic coordinates for loweringite (Gatehouse *et al.* 1978). Barium was assigned to the *A* site, manganese to the *T* (tetrahedral) and *M*(1) (octahedral) sites, and titanium to octahedral sites *M*(2) to *M*(4). Full occupancy of all metal atom sites was maintained. The trace phases rutile and ankangite (*cf.* Shi *et al.* 1991) were ignored. Refinement of the above profile-parameters, all coordinates and isotropic thermal parameters resulted in convergence at  $R_{wp} = 0.089$ ,  $R_B = 0.033$ ,

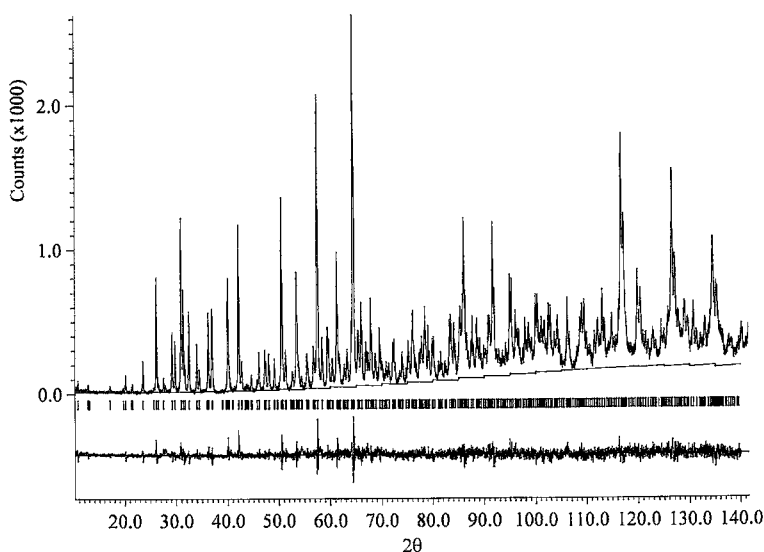


FIG. 1. The observed (broken), calculated (solid) and difference patterns for the lindsleyite data collected with a variable-time strategy.

GOF = 2.7. Figure 1 illustrates the fit of the observed and calculated patterns.

## RESULTS

### Phase studies

Table 1 summarizes the results for equilibrations of samples in a controlled atmosphere, with fixed [Ba]/[Mn+Ti] atomic ratio = 1/21, as in Ba(Mn,Ti)<sub>21</sub>O<sub>38</sub>, and with [Mn]/[Ti] ratios in the range 4/17 to 2/19. At oxygen fugacities of 10<sup>-14.5</sup> atm. or higher, lindsleyite was found to be unstable relative to

a mixture of pyrophanite (MnTiO<sub>3</sub>), rutile and a phase with a PXRD pattern the same as that reported for ankangite (Xiong *et al.* 1989, Jambor & Burke 1991). The latter is a mineral with a hollandite-related structure and with composition Ba[(Cr<sup>3+</sup>,V<sup>3+</sup>)<sub>x</sub>(Ti)<sub>8-x</sub>]O<sub>16</sub>,  $x \approx 2.5$ . Microprobe analyses of the ankangite-related phase in equilibrated samples gave typically 18.5 wt.% Ba, 47.5 wt.% Ti and 1.3 wt.% Mn, approximating to the ideal composition BaTi<sub>18</sub>O<sub>16</sub>, in which the Cr<sup>3+</sup> and V<sup>3+</sup> in ankangite are replaced by Ti<sup>3+</sup>.

At oxygen fugacities lower than 10<sup>-14.5</sup> atm., lindsleyite was found to be the dominant phase in all

TABLE 1. ACCESSORY PHASES PRESENT (FROM XRD) WITH LINDSLEYITE IN PRODUCTS FROM CONTROLLED ATMOSPHERE EQUILIBRATIONS AT 1100°C

log $f_{O_2}$	Ba:Mn:Ti atomic ratio of starting mixture				
	1 : 4 : 17	1 : 3.5 : 17.5	1 : 3 : 18	1 : 2.5 : 18.5	1 : 2 : 19
-14.5	Pyr + R + An No Lind				
-15	Pyr + An				
-15.5		Pyr + An + R(tr)	R + An	R + An	
-15.7		Pyr + An(tr)	R(tr) + An(tr)	R + An	
-16		Pyr + An	R(tr) + An(tr)	R + An(tr)	
-16.5		Pyr + An	An(tr)	RR(tr) + An(tr)	
-17.1		Pyr + An	Pyr + An(tr)	An(tr)	RR + An(tr)
-17.5		Pyr + An	Pyr + An(tr)	An(tr)	RR(tr) + An(tr)

Pyr = pyrophanite, An = ankangite, R = rutile, RR = reduced rutile, tr = trace, Lind = lindsleyite

reaction products. A trace amount of an ankangite-type phase was invariably present, indicating that the barium content of the lindsleyite was slightly less than required for the ideal  $\text{Ba}(\text{Mn},\text{Ti})_{21}\text{O}_{38}$  composition.

Compositions with  $[\text{Mn}]/[\text{Ti}]$  atomic ratios higher than 3/18 gave pyrophanite as an accessory phase over the full range of oxygen fugacities. Compositions with  $[\text{Mn}]/[\text{Ti}]$  ratios lower than 3/18 gave rutile or reduced rutile as an accessory phase, with the amount decreasing as the oxygen fugacity was lowered. At a  $[\text{Mn}]/[\text{Ti}]$  ratio of 3/18, the accessory phase changed from rutile + ankangite-type to pyrophanite + ankangite-type with decreasing oxygen fugacity. The change in the types of accessory phases with changes in bulk composition and oxygen fugacity reflect subtle changes in the composition of lindsleyite. The closest approach to a single-phase lindsleyite product occurred for  $[\text{Ba}]:[\text{Mn}]:[\text{Ti}] = 1:3:18$ , equilibrated at oxygen fugacities in the range  $10^{-15.7}$  to  $10^{-16}$  atm.

The effect of varying both  $[\text{Ba}]/[\text{Mn}+\text{Ti}]$  and  $[\text{Mn}]/[\text{Ti}]$  atomic ratios on the phase composition was studied at an oxygen fugacity of  $10^{-15.7}$  atm. The results are summarized in Table 2. By decreasing the  $[\text{Ba}]/[\text{Mn}+\text{Ti}]$  ratio below 1/21, it was possible to avoid the formation of the ankangite-related accessory phase.

Results of electron-microprobe analyses for the lindsleyite phase in samples equilibrated at an  $f(\text{O}_2)$  of  $10^{-15.7}$  atm. are reported in Table 2. The formulae calculated on a basis of 38 atoms of oxygen and 22 cations are presented. The microprobe results confirm the results of the phase studies, that there is

slightly less than one atom of barium per formula unit. Charge balance requires that about 20% of the titanium be in the trivalent state. The elemental variations shown in Table 2 are consistent with a coupled substitution of the form  $\text{Mn}^{2+} + \text{Ti}^{4+} \leftrightarrow 2 \text{Ti}^{3+}$ . Run no. 59C in Table 2 gave an almost pure lindsleyite product, with only a trace of rutile and  $\text{BaTi}_3\text{O}_{16}$  as impurities. This sample was used for the Rietveld refinement. Its formula is closely approximated by  $\text{BaMn}_3\text{Ti}_{14}^{4+}\text{Ti}_{14}^{3+}\text{O}_{38}$ .

### Refinement results

The atomic coordinates, isotropic B values and bond lengths from Rietveld refinement are given in Table 3. The mean bond-lengths for all the members of the crichtonite group are given in Table 4. Figure 2 shows the variation of the mean A-O bond-length as a function of the radii of the cations assigned to this site by the various authors. The radii are taken from Shannon (1976), and in cases where the site had not been assigned full occupancy, the radii have been calculated assuming a full site, with atoms in the same proportion as was assigned to the partially filled site. It can be seen that there is an approximately linear relationship between the assigned radii and the mean bond-length determined by structure refinement. The synthetic lindsleyite studied here has the largest mean A-O distance, which is consistent with the proposal that it contains the A-site cation with the largest ionic radius. Twelve-coordinated potassium has a slightly larger ionic radius (1.64 Å) than barium (1.61 Å), but

TABLE 2. PHASE EQUILIBRIA AT 1100°C AND  $\text{LOG } f_{\text{O}_2} = 15.7$ , TOGETHER WITH MICROPROBE ANALYSES FOR LINDSLEYITE PHASES

		Starting composition (moles)				
		59C	58C	57C	56C	55C
moles	BaO	1	0.9	0.9	1.1	1.1
	MnO	3	3.0	3.1	2.9	3.0
	TiO <sub>2</sub>	18	18.1	18	18	17.9
Accessory Phases present (by XRD)		trace rutile + trace ankangite	minor rutile	minor rutile + trace ankangite	minor ankangite	minor ankangite
Weight %	BaO	8.74	n.d.	8.12	8.17	8.43
	MnO	12.31	n.d.	12.76	13.01	13.15
	TiO <sub>2</sub>	63.37	n.d.	63.72	64.25	64.57
	Ti <sub>2</sub> O <sub>3</sub>	15.82	n.d.	14.80	14.97	14.46
	total	99.97		99.40	100.40	100.61
Atoms p.f.u.	Ba	.98		.94	.94	.97
	Mn	3.08		3.19	3.23	3.27
	Ti <sup>4+</sup>	14.0		14.12	14.17	14.23
	Ti <sup>3+</sup>	3.90		3.76	3.67	3.54

The analyses presented here are the average of two analyses for each run.  $\text{Ti}^{3+}/\text{Ti}^{4+}$  ratio has been determined assuming 22 cations and 38 oxygens per formula unit. n.d. = not determined

TABLE 3. ATOMIC COORDINATES AND BOND LENGTHS (Å),  $\text{Ti}^{3+}$ -CONTAINING LINDSLEYITE

	X	Y	Z	B(Å <sup>2</sup> )			
A	0	0	0	0.59(4)			
T	0	0	.3103(2)	0.48(6)			
M(1)	0	0	0.5	0.83(9)			
M(2)	.1860(3)	.1434(3)	.1650(2)	0.39(4)			
M(3)	.9173(4)	.2402(4)	.3926(1)	0.49(6)			
M(4)	.0714(4)	.7589(4)	.3989(1)	0.42(6)			
O(1)	.874(1)	.065(1)	.4355(5)	0.6(2)			
O(2)	.706(1)	.505(1)	.4432(5)	0.4(2)			
O(3)	.365(1)	.260(1)	.5589(4)	0.0(2)			
O(4)	.600(1)	.563(1)	.5511(5)	1.1(2)			
O(5)	.054(1)	.207(1)	.3373(6)	0.8(2)			
O(6)	.358(1)	.262(1)	.3413(5)	0.2(1)			
O(7)	0	0	.2131(8)	0.4(3)			
A-O2	x 6	2.81(1)	T-O5	x 3	2.02(1)	M(1)-O1 x6	2.21(2)
A-O6	x 6	2.93(1)	T-O7	x 1	2.09(2)		
M(2)-O2		2.052(9)	M(3)-O1		1.88(1)	M(4)-O1	1.91(1)
M(2)-O2		2.05(2)	M(3)-O2		1.91(2)	M(4)-O3	1.97(1)
M(2)-O3		1.948(9)	M(3)-O3		2.00(2)	M(4)-O4	1.84(2)
M(2)-O4		1.99(1)	M(3)-O5		2.00(1)	M(4)-O5	2.00(1)
M(2)-O4		2.03(1)	M(3)-O6		2.03(1)	M(4)-O5	2.13(2)
M(2)-O7		2.028(9)	M(3)-O6		2.06(1)	M(4)-O6	1.96(2)

TABLE 4. COMPARISON OF THE MEAN BOND-LENGTHS OF CATION POLYHEDRA

	A-O	T-O	M(1)-O	M(2)-O	M(3)-O	M(4)-O
Mathiasite 1	2.832	1.981	2.136	1.980	1.978	1.971
Mathiasite 2	2.838	1.963	2.130	1.998	1.958	1.971
Mathiasite 3	2.831	1.964	2.124	1.979	1.982	1.973
Lindsleyite	2.837	1.948	2.119	1.982	1.990	1.978
Senaité	2.817	2.012	2.227	1.998	1.976	1.964
Loveringite	2.790	1.995	2.166	1.983	1.971	1.970
Crichtonite	2.792	1.972	2.205	2.006	1.969	1.967
Davidite	2.769	1.981	2.243	2.010	1.975	1.972
Landauite	2.822	1.964	2.211	1.997	1.973	1.969
Ca <sub>2</sub> Zn <sub>2</sub> Ti <sub>10</sub> O <sub>28</sub>	2.777	1.985	2.305	2.007	1.969	1.972
present study	2.870	2.021	2.210	2.015	1.980	1.969

Mathiasite 1: Gatehouse et al. (1983); mathiasite 2: Lu & Peng (1987); mathiasite 3: Zhang et al. (1988); Ca<sub>2</sub>Zn<sub>2</sub>Ti<sub>10</sub>O<sub>28</sub>: Gatehouse & Grey (1983); lindsleyite: Zhang et al. (1988). Bond lengths expressed in Å.

the mathiasite data all pertain to natural materials, which have significant substitutions of smaller cations in the A site.

It is clear from Table 4 that the A-O and M(1)-O polyhedra show the most variation in mean bond-length. The average M(1)-O and T-O bond-lengths observed in the present study are as large as any observed in the crichtonite group of minerals, which reflects the manganese occupancy of these sites. The mean bond-lengths for the M(2), M(3) and M(4) polyhedra, which are predominantly filled with titanium, are very similar to the other minerals of the group.

### Valence sums

Bond-valence summations using parameters from Brown & Wu (1976) are reported in Table 5. The summations for the cation sites are consistent with Mn<sup>2+</sup> ordered at the T site and the large octahedral M(1) site. The trivalent titanium is ordered predominantly at the M(2) site and, to a lesser extent, at the M(3) site. The Ti<sup>3+</sup>:Ti<sup>4+</sup> ratio obtained from the bond-valence calculations is 5:13, which is close to 4:14 determined by charge balance.

Natural lindsleyite from peridotites with ΣM > 21 (Haggerty et al. 1983) may have a structure that is significantly different from that of the ordered

TABLE 5. BOND-VALENCE SUMMATION, Ti<sup>3+</sup>-BEARING LINDSLEYITE

A	2.55	O1	1.88
T	2.08	O2	2.02
M1	1.89	O3	1.90
M2	3.42	O4	2.07
M3	3.79	O5	2.12
M4	3.96	O6	1.88
		O7	2.15

Parameters A: (Ba) 7, 2.297; T and M1: (Mn<sup>2+</sup>) 5.6, 1.798; M2, M3 and M4 (Ti<sup>3+</sup>) 5.2, 1.806 (Brown & Wu 1976).

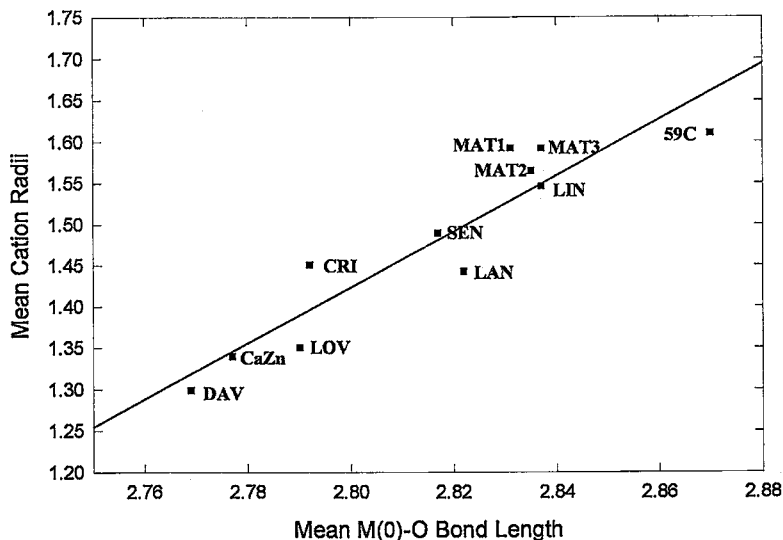


FIG. 2. The mean radii of cations occupying the A site, based on published structures, versus the mean A-O bond length. The line, a least-squares fit to the data, has a slope of 3.39 and an intercept of -8.060. See Table 4 for a key to the labels.

synthetic phase described here. It is possible that there is partial occupancy of sites, as described by Armbruster & Kunz (1990). However, temperatures and oxygen fugacities close to the iron-wüstite buffer, as used in this study, are very similar to the conditions considered to exist for some peridotites, *i.e.*, 1100°C and  $\log f(\text{O}_2)$  of  $-16$  (Arculus & Delano 1987).

The stability of lindsleyite in the system BaO–MnO–TiO<sub>2</sub>–Ti<sub>2</sub>O<sub>3</sub> at 1100°C, over the range of oxygen fugacities normally encountered in Becher-type upgrading of ilmenite, presents the possibility that Ra<sup>2+</sup> daughters from radionuclide impurities could segregate into this type of phase. In the SREP process involving flux addition, lindsleyite could form solid solutions with other crichtonite-group end members containing alkali and alkaline earth A cations derived from the flux.

#### ACKNOWLEDGEMENTS

The authors thank L. Cranswick, C. Li and I. Harrowfield for help with X-ray analysis, synthesis and microprobe analysis, respectively. Reviews by Dr. S. Haggerty and an anonymous reviewer improved the manuscript. This work was financed in part by an N.S.E.R.C. operating grant to R.C.P.

#### REFERENCES

- ARCULUS, R.J. & DELANO, J.W. (1987): Oxidation state of the upper mantle: present conditions, evolution, and controls. *In* *Mantle Xenoliths* (P.H. Nixon, ed.). John Wiley & Sons, New York, N.Y. (589-598).
- ARMBRUSTER, T. & KUNZ, M. (1990): Cation arrangement in an unusual uranium-rich senaite: crystal structure study at 130 K. *Eur. J. Mineral.* **2**, 163-170.
- BECHER, R.G., CANNING, R.G., GOODHEART, B.A. & UUSNA, S. (1965): A new process for upgrading ilmenitic mineral sands. *Proc. Aust. IMM* **214**, 21-44.
- BROWN, I.D. & WU, KANG KUN (1976): Empirical parameters for calculating cation–oxygen bond valences. *Acta Crystallogr.* **B32**, 1957-1959.
- BUYKX, W.J., HAWKINS, K., LEWIS, D.M., MITAMURA, H., SMART, R., STEVENS, G.T., WATSON, K.G., WEEDON, D. & WHITE, T.J. (1988): Titanite ceramics for the immobilization of sodium-bearing high-level nuclear waste. *J. Am. Ceram. Soc.* **71**, 678-688.
- CAGLIOTI, G., PAOLETTI, A. & RICCI, F.P. (1958): Choice of collimators for a crystal spectrometer for neutron diffraction. *Nucl. Instrum.* **3**, 223-228.
- ELLIS, B.A., HARRIS, H.R. & HUDSON, R.L. (1994): The reduction of radionuclides in titaniferous feedstocks. Proc. 11th Industrial Minerals Int. Congress, Berlin, Germany.
- GATEHOUSE, B.M. & GREY, I.E. (1983): The crystal structure of Ca<sub>2</sub>Zn<sub>4</sub>Ti<sub>16</sub>O<sub>38</sub>. *J. Solid State Chem.* **46**, 151-155.
- , —————, CAMPBELL, I.H. & KELLY, P.R. (1978): The crystal structure of loveringite, a new member of the crichtonite group. *Am. Mineral.* **63**, 28-36.
- , ————— & KELLY, P.R. (1979): The crystal structure of davidite. *Am. Mineral.* **64**, 1010-1017.
- , ————— & SMYTH, J.R. (1983): Structure refinement of mathiasite (K<sub>0.62</sub>Na<sub>0.14</sub>Ba<sub>0.14</sub>Sr<sub>0.10</sub>)<sub>Σ1.0</sub> [Ti<sub>12.90</sub>Cr<sub>3.10</sub>Mg<sub>1.53</sub>Fe<sub>2.15</sub>Zr<sub>0.67</sub>Ca<sub>0.29</sub>(V,Nb,Al)<sub>0.36</sub>]<sub>Σ21</sub>O<sub>38</sub>. *Acta Crystallogr.* **C39**, 421-422.
- GREY, I.E. & GATEHOUSE, B.M. (1978): The crystal structure of landauite, Na{MnZn<sub>2</sub>(Ti,Fe)<sub>6</sub>Ti<sub>12</sub>}O<sub>38</sub>. *Can. Mineral.* **16**, 63-68.
- , LI, C. & REID, A.F. (1974): A thermodynamic study of iron in reduced rutile. *J. Solid State Chem.* **11**, 120-127.
- & LLOYD, D.J. (1976): The crystal structure of senaite. *Acta Crystallogr.* **B32**, 1509-1513.
- , ————— & WHITE, J.S., JR. (1976): The crystal structure of crichtonite and its relationship to senaite. *Am. Mineral.* **61**, 1203-1212.
- & REID, A.F. (1974): Reaction sequences in the reduction of ilmenite. 3. Reduction in a commercial rotary kiln; an X-ray diffraction study. *Trans. Inst. Mining Metall.* **83**, C39-46.
- HAGGERTY, S.E. (1975): The chemistry and genesis of opaque minerals in kimberlites. *Phys. Chem. Earth* **9**, 295-307.
- , SMYTH, J.R., ERLANK, A.J., RICKARD, S.R. & DANCHIN, R.V. (1983): Lindsleyite (Ba) and mathiasite (K): two new chromium-titanates in the crichtonite series from the upper mantle. *Am. Mineral.* **68**, 494-505.
- HILL, R.J. & HOWARD, C.J. (1986): A computer program for Rietveld analysis of fixed-wavelength X-ray and neutron powder diffraction patterns. *Aust. Atomic Energy Comm. Rep.* **M112**.
- INTERNATIONAL TABLES FOR X-RAY CRYSTALLOGRAPHY (1974): Vol. IV. The Kynoch Press, Birmingham, England.
- JAMBOR, J.L. & BURKE, E.A. (1991): New mineral names. *Am. Mineral.* **76**, 2020-2026.
- JIAJI JIANG, JIANHONG ZHANG & JIANGUO MA (1990): Mössbauer spectroscopy and crystallochemistry of lindsleyite–mathiasite. *Acta Mineral. Sinica* **10**, 370-375 (in Chinese).
- QI LU & ZHIZHONG PENG (1987): Crystal structure of mathiasite. *Acta Petrologica et Mineralogica* **6**, 221-229 (in Chinese).
- MADSEN, I.C. & HILL, R.J. (1994): Collection and analysis of powder diffraction data with near constant counting statistics. *J. Appl. Crystallogr.* **27**, 385-392.

- RIETVELD, H.M. (1969): A profile refinement method for nuclear and magnetic structures. *J. Appl. Crystallogr.* **2**, 65-71.
- SHANNON, R.D. (1976): Revised effective ionic radii and systematic studies of interatomic distances in halides and chalcogenides. *Acta Crystallogr.* **A32**, 751-767.
- NICHENG SHI, ZHESHENG MA & WEI LIU (1991): Crystal structure determination of ankangite with one-dimensional incommensurate modulation. *Acta Petrol. Mineral.* **10**(8), 233-245 (in Chinese, English abstr.).
- SUZUKI, K. & SAMBONGI, K. (1972): High temperature thermodynamic properties in the Ti-O system. *Tetsu-to-Hagane* **58**, 1579-1593 (in Japanese).
- WILES, D.B. & YOUNG, R.A. (1981) : A new computer program for Rietveld analysis of X-ray powder diffraction patterns. *J. Appl. Crystallogr.* **14**, 149-151.
- MING XIONG, ZHE-SHENG MA & ZHIZHONG PENG (1989): A new mineral - ankangite. *Chinese Sci. Bull.* **34**, 592-596 (in Chinese).
- JIANHONG ZHANG, LIANGJING LI & JIANGUO MA (1989): The lindsleyite-mathiasite series in kimberlite from Shandong province. *Acta Mineral. Sinica* **9**, 25-32 (in Chinese).
- JIANHONG ZHANG, JIANGUO MA & LIANGJING LI (1988): The crystal structures and crystal chemistry of lindsleyite and mathiasite. *Geological Review* **34**, 132-144 (in Chinese).

Received June 20, 1994, revised manuscript accepted June 2, 1995.